Ultrafast Time-Resolved Soft X-Ray Photoelectron Spectroscopy of Dissociating Br_2

Lora Nugent-Glandorf, Michael Scheer,* David A. Samuels, Anneliese M. Mulhisen,
Edward R. Grant,† Xueming Yang,‡ Veronica M. Bierbaum, and Stephen R. Leone§
JILA, National Institute of Standards and Technology and Department of Chemistry and Biochemistry,
Department of Physics, University of Colorado, Boulder, Colorado 80309-0440
(Received 21 May 2001; published 22 October 2001)

The dissociation of excited state Br_2 is probed with the novel technique of ultrafast soft x-ray photoelectron spectroscopy. Excited Br_2 molecules are prepared in the dissociative $^1\Pi_u$ state with 80 fs, 400 nm pulses, and a series of photoelectron spectra are obtained during dissociation with pulses of soft x-ray light (47 nm, 26.4 eV, 250 fs). The formation of Br atoms is readily detected and the data support an extremely fast dissociation time for Br_2 on the order of 40 fs. Amplitudes of the pump-probe features reveal that the ionization cross section of atomic Br at 47 nm is ~40 times larger than that of Br_2.

DOI: 10.1103/PhysRevLett.87.193002 PACS numbers: 33.80.Eh, 33.60.Cv, 42.65.Ky, 42.65.Re

The progress of ultrafast laser spectroscopy in recent years has been remarkable, and many previously unexplored phenomena are being investigated in atoms, molecules, and condensed phase systems. These include Rydberg wave packets in atoms [1], molecular wave packets [2], coherent control of molecular systems [3,4], molecular charge transfer [5], dynamics of caged negative ions [6,7], dissociation dynamics via multiphoton excitation [8], and ultrafast reactions and electron dynamics on surfaces [9]. In light of these advances, the possibility for new ways to monitor a chemical reaction in real time, whether on a surface or in the gas phase, is a topic of increasing interest. As a chemical bond is broken (or made), the electron distribution changes on an ultrafast time scale to accommodate the moving nuclei. To understand how this electron distribution changes with time is not only of fundamental importance but will also provide critical information on the specific chemical system and the dynamics of the ensuing reaction.

To probe the dynamics of ultrafast chemical processes of neutral molecules in the gas phase we present here a novel femtosecond pump-probe experiment utilizing a visible pump pulse (400 nm) and a soft x-ray (47 nm) probe pulse. High-order harmonic generation in rare gases is used to produce ultrafast, coherent, soft x-ray radiation, which is applied to obtain photoelectron spectra of Br_2 molecules as they dissociate. The changing electron distribution of the dissociating molecule is reflected in the binding energies of the electrons themselves and thus is detectable in its valence and core level soft x-ray photoelectron spectra. For the first time, these experiments extend the field of x-ray photoelectron spectroscopy of neutral molecules to the ultrafast time domain. In a simple excitation scheme,

$$Br_2(X^1\Sigma_g^+) \xrightarrow{400\text{ nm}} Br_2^*(C^1\Pi_u) \rightarrow 2Br(^2P_{3/2}),$$

$$Br_2 \quad \text{or} \quad Br \xrightarrow{47\text{ nm}} Br_2^+(X,A,B) \quad \text{or} \quad Br^+(^3P_{2,1,0}) + e^-,$$

we observe a real time signature of a bond breaking in a gas phase molecule by measuring the kinetic energies of the ejected electrons as a function of pump-probe time delay.

Recent advances in high-harmonic generation techniques have led to other new photoelectron spectroscopy experiments utilizing femtosecond visible or UV-pump wavelengths and soft x-ray probe wavelengths. The first time-resolved experiments using soft x-ray probe light pulses were reported by Probst and Haight [10], who studied electron-phonon interactions on the surface of organic thin films. In related experiments, a cross correlation was obtained between a visible and a harmonic pulse by monitoring the signal from very fast (≤20 fs) hot-electron relaxation dynamics on a Pt surface [11]. Evidence of a change in the chemical environment of oxygen on a Pt surface was observed in a visible-excite harmonic-probe photoelectron experiment [12].

While previous work has used high harmonics to probe surface dynamics where high target densities ensure substantial photoelectron signals, here we demonstrate the applicability of femtosecond soft x-ray pulses for low-density gas phase pump-probe spectroscopy. The instrument, based on high-order harmonic generation, is described in more detail in Ref. [13]. Of the initial 1 kHz, 80 fs, 2.2 mJ Ti:sapphire laser, ~1.7 mJ is focused to an intensity of 5×10^{14} W/cm^2 in a 1 kHz pulsed gas jet of Ar to generate coherent, ultrafast, high-order harmonics in the soft x-ray region. For the present experiment, the 17th harmonic of 800 nm (26.4 eV, 47 nm) is selected and refocused with a pair of grazing-incidence gratings (one spherical and one toroidal) to probe the valence electron distribution of Br_2 during dissociation. The photon flux of the soft x-ray light is estimated from known ionization cross sections of Xe 5p lines [14] to be $\sim 3 \times 10^6$ photons/pulse at the 17th harmonic. A pair of gratings is utilized to minimize the otherwise significant pulse stretching due to pulse front tilt with some remaining linear chirp. The final temporal width of the 17th harmonic pulse is measured by above-threshold ionization (ATI) cross correlation with the 80 fs, 400 nm pulses in Xe to be ~290 fs FWHM [15,16]. ATI is a technique where the visible photon energy is added to the photon energy of the 17th harmonic when the pulses are overlapped spatially and temorally ($t = 0$).

Approximately 20% of the Ti:sapphire beam is frequency doubled in a 0.1 mm thick BBO crystal with a conversion efficiency of ~40%. The 400 nm pulse is then used to pump the Br_2 molecule into the $^1\Pi_u$ dissociative state. Before high-harmonic generation, the probe beam passes through a 1 μm precision delay stage. The 400 and 47 nm beams are overlapped spatially after passing through a 1 mm slit located 5 cm before the interaction region. The gaseous Br_2 sample is leaked into the chamber through a 0.3 mm diameter nozzle opening from a glass ampule containing ~1 mL of the liquid. The background pressure in the vacuum chamber is 6.7×10^{-6} Pa (5×10^{-8} Torr) and rises to 6.7×10^{-3} Pa (5×10^{-5} Torr) during experiments. Electrons are energy resolved in a time-of-flight magnetic bottle electron spectrometer and collected with a microchannel plate (MCP) detector.

Figure 1 gives the potential energy curve diagram of Br_2/Br_2^+ taken from Refs. [17] and [18]. This simplified diagram illustrates four different processes that are observed in the data presented here. These include (1) the background signal from ground state ionization by the 17th harmonic, (2) the cross-correlation signals at $t = 0$, (3) ionization of the excited state wave packet before dissociation is complete, and (4) the ionization of the final Br atom products. These different processes are discussed in more detail below.

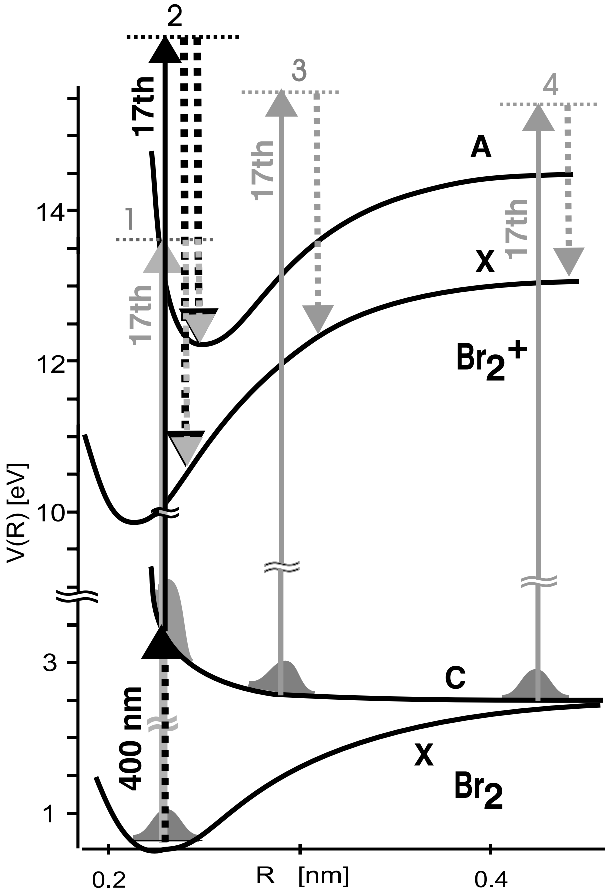

FIG. 1. A simplified potential curve diagram illustrating the pump-probe sequence (upward arrows) and resulting photoelectrons (downward arrows). Process 1: ground state absorption of the 17th harmonic (B ion state not shown). Process 2: two photon ionization with the 400 nm + the 17th harmonic centered at $t = 0$. Process 3: ionization with the 17th harmonic from the excited C state of Br_2^* at a positive time delay (but before dissociation is complete). Process 4: after complete dissociation, the Br atoms are ionized by the 17th harmonic. The total energy of the probe laser is decreased for simplicity and size of the diagram.

The valence level photoelectron spectrum of Br_2 taken with the 17th harmonic of 800 nm is shown in Fig. 2(a). The three final electronic states of the molecular ion accessible with this photon energy are observed. The solid lines in Fig. 2(a) indicate the known binding energies of the Br^+ atomic states [19]. Figure 2(b) expands three pump-probe spectra from the dotted box in Fig. 2(a), corresponding to pump-probe delays of −500, −100, and +500 fs. All photoelectron spectra are plotted as a function of binding energy, which is defined as $h\nu_{47\ \mathrm{nm}}$—photoelectron energy. With this convention, the background and atomic signals coming from a one-photon ionization appear at the correct atomic and molecular binding energies, while two-photon signals [process (2) in Fig. 1] are shifted by the energy of a 400 nm photon. The spectrum corresponding to $\Delta t = -500$ fs is the background signal that appears with the soft x-ray pulse coming before the 400 nm pump pulse. The signal in the $\Delta t = -100$ fs spectrum at 7.5 eV binding energy is indicative of a cross correlation, by means of a two-photon ionization (400 nm + 17th harmonic pulses) in Br_2. This signal can originate in two ways: (i) the 400 nm pulse promotes the wave packet resonantly to the excited state and is instantaneously ionized by the 17th harmonic or (ii) an ATI process occurs where the 400 nm photon energy is added to that of the 17th harmonic. Since the dissociating wave packet is observed directly by other means (discussed later in this work), it is likely that some combination of the two processes is responsible. Cross-correlation features are also expected where the Br_2^+ is produced in the A and B states. The A state cross-correlation signal appears as a small shoulder on the low binding energy side of the X state background peak and the B state signal is expected to be of a similar binding energy as the atomic signal, further complicating the spectrum. Last, in the $\Delta t = +500$ fs spectrum, photoelectron peaks from the Br atom are observed at the expected binding energies while the cross-correlation signal is no longer present. This atomic signal persists at long time delays ($\Delta t = 100$ ps) compared to the time scale of the dissociation dynamics ($\Delta t = <500$ fs).

In Figs. 3(a) and 3(b), several photoelectron spectra are normalized and the background molecular signal is subtracted so that only the time-correlated signal remains. Figures 3(a) and 3(b) show a series of pump-probe spectra in the relevant energy ranges where the time-correlated peaks appear. The small shift of the photoelectron spectra

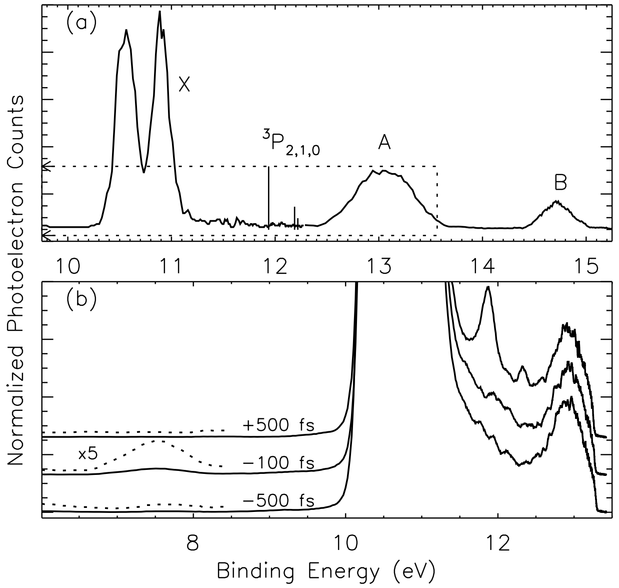

FIG. 2. (a) The photoelectron spectrum of gaseous Br_2 at 5×10^{-5} Torr taken with the 17th harmonic of 800 nm showing the final X, A, and B states of the Br_2^+ ion. Solid black lines denoted $^3P_{2,1,0}$ are the known binding energies of the bare Br atom. (b) Three pump-probe spectra of Br_2: $\Delta t = -500$ fs (background), -100 fs (cross-correlation signal), and $+500$ fs (Br atom signal). A rise in the background noise from (a) is due to saturation of the detector on the main peak in order to amplify the small pump-probe signal. The spectra are displaced vertically for clarity.

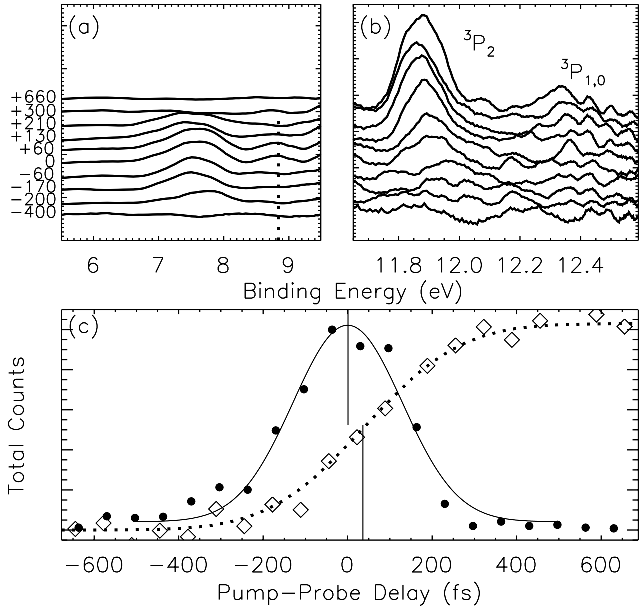

FIG. 3. (a) Normalized, subtracted pump-probe spectra of Br_2 in the cross-correlation time region. The spectra are displaced vertically for clarity. Numbers on the vertical scale are pump-probe delay in femtoseconds. The dotted line highlights a small photoelectron signal possibly arising from the dissociating Br_2 molecule. (b) Appearance of the Br atom peak in the photoelectron spectra. The two peaks in the photoelectron spectrum are due to spin-orbit coupling in the final Br^+ state. (c) Total counts from (a) and (b) and additional time delay data not shown are plotted as a function of pump-probe delay. The cross-correlation signal is fit to a Gaussian function of width ~300 fs and the atomic rise is fit with a step function described in the text.

to lower binding energies with increasing time delay is the result of a linear chirp in the soft x-ray pulse that is not compensated by the grating pair. From the data, it is clear that the atomic peaks rise very quickly, although their onset is delayed slightly with respect to the cross correlation. This is more clearly seen in Fig. 3(c) where the total photoelectron counts under both the cross-correlation peak and the atomic peaks are plotted vs pump-probe delay. The solid line represents a Gaussian fit to the cross-correlation data points (filled circles) with a full width at half maximum of 300 ± 14 fs and peak time $t_0 = 0 \pm 14$ fs. The dotted line is a fit to the rise of the total atomic signal (diamonds) with a smoothed step function given by the following equation:

$$S(t) = \frac{1}{2}\,\mathrm{erf}\left(\frac{(t - \tau_{\mathrm{step}})2\sqrt{\ln 2}}{\sigma_{\mathrm{FWHM}}}\right) + \frac{1}{2}\,. \qquad (1)$$

$S(t)$ is the total signal, τ_{step} is the average time delay between a hypothetical instantaneous photon absorption and product atom formation, and σ_{FWHM} is the full width at half maximum of the above mentioned Gaussian [20]. The best fit to the data was found with $\sigma_{\mathrm{FWHM}} = 250 \pm 14$ fs and $\tau_{\mathrm{step}} = 40 \pm 14$ fs.

This 40 fs delay of the onset of the atomic signal with respect to the center of the cross correlation suggests a very fast dissociation time for the Br_2 molecule. From an estimate of the shape of the dissociative $^1\Pi_u$ curve, a total energy calculation reveals that in 40 fs the Br-Br separation will have reached ~3 Å from an initial equilibrium bond distance of $R_e = 2.23$ Å in the ground state [17]. This elongated bond distance is in a regime where atomic behavior cannot be ruled out, but it is still closer to R_e than $2R_e$, a bond distance where it is safe to assume the bond is completely broken. Shortly after the two pulses begin to overlap, there is always some percentage of the soft x-ray probe pulse that follows the much shorter 400 nm pump pulse. With an estimated dissociation time of ≤40 fs, some signal due to atoms in the interaction region should appear at very early time delays. However, one might also expect a broad peak in the atomic region at early time delays, with signal coming from the dissociating wave packet over several regions of the dissociative curve. Then at later time delays, the atomic peak should become narrower as the dissociation is nearly complete. The results presented in Fig. 3 show no visible broadening of the atomic peak at early time delays. However, such a broadening of the signal could be wider than 1 eV considering the energy scale covered by the $^1\Pi_u$ curve and might be impossible to detect above the background parent molecule signal level [see Fig. 2(b)].

The analysis of the dissociative state photoelectron spectra is complicated by multiple final states of the ion and multiple cross-correlation features. If the ion is left in the X state after ionization at a dissociative bond distance of ~2.4 Å, a photoelectron peak between the two observed cross-correlation peaks (that leave the Br_2^+ in the X state and the A state) is expected. The small peak indicated by the dotted line in Fig. 3(a) at ~8.75 eV binding energy could arise from the dissociating wave packet. This signal rises and decays on the appropriate time scale for it to be a dissociative state photoelectron feature. Another explanation of the observations is the possible existence of an ion-induced dipole potential curve that would almost mirror the neutral dissociative curve, except with a very shallow well. This could cause the photoelectron feature arising from the dissociating wave packet to appear at a nearly constant energy. This could account for the nonshifting atomiclike peak that is observed. A more rigorous theoretical treatment of this problem and improved signal to noise are desired for a finalized interpretation of the data.

Another important result is the obvious difference in the ionization cross section between the bromine molecule and the atom at the 47 nm probe wavelength. From the reported absorption cross section of neutral Br_2 [21] and laser energy at 400 nm, an estimated 0.02% of the molecules in the interaction region reach the excited dissociative state, leaving the rest in the ground state. By comparing a background photoelectron spectrum to a pump-probe spectrum at long time delays [corresponding to the -500 fs and $+500$ fs spectra in Fig. 2(b)], it is possible to calculate the ratio of the increase of the atomic signal versus the corresponding decrease in background molecular signal (due to depletion of the ground state). An analysis of the total counts reveals that the probe wavelength is ~40 times more sensitive to the atoms than to the ground state molecule (taking into account the stoichiometric ratio of Br_2 to Br). Note the area under the peaks in Fig. 2 is not representative of the total counts used in the calculation, because the A state appears compressed on the energy scale. Since the intensities of the 400 nm pump beam are close to the multiphoton regime, the effects of a multiphoton pump step on the interpretation of the data presented here are also under investigation. An important scientific question is whether the cross section of the dissociative molecular state is similarly enhanced. If not, a broad signal originating from the dissociative state of the molecule in the atomic photoionization energy region may be easily obscured.

In conclusion, we show a series of ultrafast photoelectron spectra of the gas phase dissociation of Br_2 obtained with a 400 nm pump pulse and a soft x-ray probe pulse. Key results point to challenging new problems involving the cross sections and shapes of photoelectron features arising from dissociating states, as well as understanding the role of cross-correlation processes versus dissociative wave packet signals. UV-pump/soft x-ray probe photoelectron spectroscopy promises to offer a unique and powerful way to probe the dissociation dynamics of neutral molecules in the gas phase on ultrafast time scales.

The authors gratefully acknowledge funding from the U.S. AFOSR, with additional equipment and support from NSF and NIST. L. N.-G. and D. S. acknowledge support from OSEP, also funded by NSF. M. S. thanks the NSERC of Canada for funding. E. G. also acknowledges support from NSF. We also thank the staff of the JILA instrument and electronic shops for their expert involvement in this project.

---

*Present address: Nortel Networks, MS 04332F15, Nepean, Ontario, Canada, K2H 8E9.

†JILA Visiting Fellow.
Permanent address: Department of Chemistry, Purdue University, West Lafayette, IN 47907.

‡JILA Visiting Fellow.
Permanent address: Institute of Atomic and Molecular Sciences, Academia Sinica, Taipei, Taiwan.

§Also Quantum Physics Division, National Institute of Standards and Technology.

[1] J. C. Diels and W. Rudolph, *Ultrashort Laser Pulse Phenomena* (Academic Press, San Diego, 1996), p. 446.
[2] R. M. Bowman, M. Dantus, and A. H. Zewail, Chem. Phys. Lett. **161**, 297 (1989).
[3] R. Uberna, Z. Amitay, R. Loomis, and S. R. Leone, Faraday Discuss. **113**, 385 (1999).
[4] J. Ahn, T. C. Weinacht, and P. H. Bucksbaum, Science **287**, 463 (2000).
[5] S. Lochbrunner, T. Schultz, M. Schmitt, J. P. Shaffer, M. Z. Zgierski, and A. Stolow, J. Chem. Phys. **114**, 2519 (2001).
[6] A. Sanov, T. Sanford, S. Nandi, and W. C. Lineberger, J. Chem. Phys. **111**, 664 (1999).
[7] B. J. Greenblatt, M. T. Zanni, and D. M. Neumark, Science **276**, 1675 (1997).
[8] J. A. Davies, J. E. LeClaire, R. E. Continetti, and C. Hayden, J. Chem. Phys. **111**, 1 (1999).
[9] W. Z. Line, R. W. Schoenlein, J. G. Fujimoto, and E. P. Ippen, IEEE J. Quantum Electron. **24**, 267 (1988).
[10] M. Probst and R. Haight, Appl. Phys. Lett. **71**, 202 (1997).
[11] P. Siffalovic *et al.,* Rev. Sci. Instrum. **72**, 30 (2001).
[12] M. Bauer, C. Lei, K. Read, R. Tobey, M. Murnane, and H. C. Kapteyn, Phys. Rev. Lett. **87**, 025501 (2001).
[13] L. Nugent-Glandorf, M. Scheer, M. Krishnamurthy, J. W. Odom, and S. R. Leone, Phys. Rev. A **62**, 023812 (2000).
[14] D. W. Turner, C. Baker, A. D. Baker, and C. R. Brundle, *Molecular Photoelectron Spectroscopy* (John Wiley and Sons Ltd., London, 1970), p. 43.
[15] A. Bouhal *et al.,* J. Opt. Soc. Am. B **14**, 950 (1997).
[16] T. E. Glover, R. W. Schoenlein, A. H. Chin, and C. V. Shank, Phys. Rev. Lett. **76**, 2468 (1996).
[17] A. B. Peterson and I. W. M. Smith, Chem. Phys. **30**, 407 (1977).
[18] G. Herzberg, *Molecular Spectra and Molecular Structure: Spectra of Diatomic Molecules* (Prentice-Hall, New York, 1939).
[19] K. Kimura, T. Yamazaki, and Y. Achiba, Chem. Phys. Lett. **58**, 104 (1978).
[20] J. E. Kim, D. W. McCamant, L. Shu, and R. A. Mathies, J. Phys. Chem. B **105**, 1240 (2001).
[21] S. Hubinger and J. B. Nee, J. Photochem. Photobiol. A **86**, 1 (1995).